https://doi.org/10.5194/amt-2021-382
Preprint. Discussion started: 3 December 2021

Atmospheric Measurement Techniques Discussions

Quantification of major particulate matter species from a single filter type using infrared spectroscopy – Application to a large-scale monitoring network

Bruno Debus[1], Andrew T. Weakley[1], Satoshi Takahama[2], Kathryn M. George[1,3], Bret Schichtel[4], Scott Copeland[5], Anthony S. Wexler[1,6], Ann M. Dillner[1]*

[1] Air Quality Research Center, University of California, Davis, California, 95616, USA

[2] ENAC/IIE, Swiss Federal Institute of Technology Lausanne (EPFL), Lausanne, Switzerland

[3]Monitoring and Laboratory Division, California Air Resources Board, Sacramento, CA 95811, USA

[4]National Park Service, Cooperative Institute for Research in the Atmosphere, Colorado State University, Fort Collins, CO 80523, USA

[5] Cooperative Institute for Research in the Atmosphere, Colorado State University, Fort Collins, CO, 80523, USA

[6]Departments of Mechanical and Aerospace Engineering, Civil and Environmental Engineering, and Land, Air and Water Resources, University of California, Davis, California, 85616, USA

Correspondence to: Ann M. Dillner (amdillner@ucdavis.edu)

Abstract

To enable chemical speciation, monitoring networks collect particulate matter (PM) on different filter media, each subjected to one or more analytical techniques to quantify PM composition present in the atmosphere. In this work, we propose an alternate approach that uses one filter type (teflon or polytetrafluoroethylene, PTFE, commonly used for aerosol sampling) and one analytical method, Fourier Transform Infrared (FT-IR) spectroscopy to measure almost all of the major constituents in the aerosol. In the proposed method, measurements using the typical multi-filter, multi-analytical techniques are retained at a limited number of sites and used as calibration standards while sampling on PTFE and analysis by FT-IR is solely performed at the remaining locations. This method takes advantage of the sensitivity on the mid-IR domain to various organic and inorganic functional groups and offers a fast and inexpensive way of exploring sample composition. As a proof of concept, multiple years of samples collected within the Interagency Monitoring of PROtected Visual Environment network (IMPROVE) are explored with the aim of retaining high quality predictions for a broad range of atmospheric compounds including total mass, organic (OC), elemental (EC) and total (TC) carbon, sulfate, nitrate and

https://doi.org/10.5194/amt-2021-382
Preprint. Discussion started: 3 December 2021

Atmospheric Measurement Techniques Discussions

crustal elements. Findings suggest that models based on only 21 sites, covering spatial and seasonal trends in atmospheric composition, are stable over a three year period within the IMPROVE network with prediction accuracy (R^2 > 0.9, median bias less than 3% for most constituents. Incorporating additional sites at low cost or partially replacing existing, more time and cost intensive techniques are among the potential benefits of one-filter, one-method approach.

https://doi.org/10.5194/amt-2021-382
Preprint. Discussion started: 3 December 2021


Atmospheric Measurement Techniques Discussions

1 Introduction

In the United States, filter-based chemical speciation of ambient aerosols has been in operation for decades to quantify trends, assess transport and atmospheric transformation, identify sources of air pollution, evaluate impacts of pollution regulations, assess impacts on visibility, radiative forcing, human and ecosystem health and evaluate atmospheric and climatological models. The two federally funded speciation networks, the Interagency Monitoring of PROtected Visual Environments (IMPROVE) and the Chemical Speciation Network (CSN) collect 24-hour filter samples using three filter media: polytetrafluoroethylene for analysis by gravimetry, hybrid integrating plate and sphere (HIPS), and x-ray fluorescence (XRF), quartz for thermal optical reflectance (TOR) and nylon for ion chromatography. Over the decades of operation, the analytical methods have evolved with efforts to maintain consistency in trends while also adopting improved methodology and retiring obsolete equipment. Impacts of many of these changes have been addressed in the literature (Hyslop et al., 2015, 2012; White et al., 2016; Zhang et al., 2021; Chow et al., 2007a, 2015) and in data advisories posted on the IMPROVE website (http://vista.cira.colostate.edu/Improve/data-advisories/).

In this paper, we explore the use of Fourier transform-infrared spectroscopy (FT-IR) to reproduce most of the existing speciation data because the most components exhibit optical activity in the mid-IR. The number and bands of organic compounds are numerous, but generally group frequencies can be found above 1500 cm^{-1} and compound-specific spectral patterns ("fingerprint region") below this frequency; down to approximately 700 cm^{-1} (for example,(Weakley et al., 2016; Mayo et al., 2004). Graphitic carbon displays peaks near 1600 cm^{-1} due to lattice defects (Tuinstra and Koenig, 1970; Friedel and Carlson, 1971), displacement vibrations near 868 cm^{-1} (Nemanich et al., 1977), and a broad, sloping absorbance between 4000 and 1500 cm^{-1} due to the tail of the electronic transition more strongly observed in the UV (Parks et al., 2021). Inorganic substances containing polyatomic ions such as sulfate, nitrate, and ammonium have strong vibrational modes above 600 cm^{-1} (Mayo, 2004). Crystalline and amorphous geological minerals in the form of oxides (which include hydroxides and oxyhydroxides) have distinct internal vibrational modes influenced by the electronegativity of the metal to which the oxygen is bonded (Busca and Resini, 2006; Chukanov and Chervonnyi, 2016; Margenot et al., 2017).

FT-IR spectra with partial least squares (PLS) calibrations have been shown to reproduce OC and EC concentrations using organic and graphitic carbon absorption bands, respectively, at a limited number of sites in the IMPROVE network (Dillner and Takahama, 2015a, b; Reggente et al., 2016), CSN (Weakley et al., 2016, 2018a) and FRM (Weakley et al., 2018b). Takahama et al. (2019) reviews these findings and the overall framework to be used for the two phases of such statistical calibrations: model building (sample selection, spectral preparation, model generation, model selection, model evaluation, and model understanding) and operation (error anticipation and model updating). Inorganic ions and geological mineral absorption bands have been used for

https://doi.org/10.5194/amt-2021-382
Preprint. Discussion started: 3 December 2021


Atmospheric Measurement Techniques Discussions

chemical speciation of these substances using FT-IR in prior studies (e.g., Cunningham et al., 1974; McClenny et al., 1985; Pollard et al., 1990; Bogard et al., 1982; Foster and Walker, 1984).

Organic absorption bands are useful for measuring OC but also provide spectral information needed to add detailed knowledge of composition not currently measured in air quality monitoring networks – such as organic matter (OM) and organic functional group composition – which is the subject of other work (Reggente et al., 2019; Boris et al., 2019, 2021; Burki et al., 2020). Such calibrations, also combined with factor analytic approaches, can provide source characterization on par with more costly mass spectrometric techniques (Boris et al., 2021; Yazdani et al., 2021a; Hawkins et al., 2010; Takahama et al., 2011; Liu et al., 2012; Corrigan et al., 2013).

Although FT-IR shows promise for measuring many constituents in aerosol, it is not without its challenges. One limitation is that not all PM constituents can be measured, or measured with high sensitivity, from the FT-IR spectrum. For instance, NaCl and $MgCl_2$ do not have IR-active substituents. While a multitude of spectral signatures associated with mineral dust arise from their constituent bonds – e.g., the metal-oxygen bonds in oxides (the oxide form is explicitly assumed in estimating dust mass concentrations from elemental composition for the IMPROVE network), some must be predicted from correlation with other constituents (e.g., some forms of iron) if IR-activity is lacking. Other substances are IR-active but have weak responses, such as graphitic carbon (Niyogi et al., 2006; Parks et al., 2021). The absorption and scattering by the PTFE filter also pose challenges for quantitative analysis. The PTFE-based material changes over time due to change in manufacturer or manufacturing process, and is difficult to fully characterize a priori or treat with simple blank subtraction techniques. PTFE absorption limits full access to the range of spectroscopic information in the mid-IR, for instance in the region of carbon-oxygen bonds that can lead to less than full recovery of OM mass. Additionally, scattering leads to broadly-varying slope in the group frequency region. This scattering artifact is minimized by baselining (Kuzmiakova et al., 2016) and using many standards that have a range of scattering and absorption observed in the network (Debus et al., 2019), yet these techniques can still lead to errors in quantification. Weakley et al., (2018b) demonstrated that calibrations built using one brand of filter can be accurately extended to another brand of PTFE filter with numerically marginal but statistically significant increase in method error (e.g., +2% error for α=0.05). However, these studies are insufficient to generalize findings to all types of sampling filters.

The goal of this work is to assess the capability of using FT-IR to measure the aerosol chemical composition at all IMPROVE sites. FT-IR quickly and non-destructively collects information-rich spectra from routinely collected PTFE filter samples. Ambient samples from strategically-selected IMPROVE sites are used for calibration and reasonably mimic the composition, matrix effects and substrates of the unknowns, all of which theoretically lead to accurate estimations of concentrations. Using all samples from selected sites reduces maintenance, shipping, processing

https://doi.org/10.5194/amt-2021-382
Preprint. Discussion started: 3 December 2021


Atmospheric Measurement Techniques Discussions

and coordinating required to maintain intermittent quartz and nylon filter sampling at every site. Sites are selected using data from 2015 and are used for calibrating samples from 2015-2017. Samples from all other (non-calibration) IMPROVE sites are predicted and compared to routine IMPROVE data to assess the quality of prediction. Aerosol components to be measured include TC, OC, EC, inorganic ions, soil elements, particulate mass, and light absorption.

2 Methods

2.1 Network data

IMPROVE samples collected every third day at all North American sites (Section S1) from January 2015 through December 2017 are included in this study. Fine particulate matter (aerodynamic diameter less than 2.5 micrometers) is deposited on 25 mm diameter filters polytetrafluoroethylene (PTFE) and quartz filters by sampling air at a nominal flowrate of 22.8 liters per minute from midnight to midnight local time. Parallel 37 mm nylon filters are collected at the same flow flowrate. PTFE filters are analyzed by multiple instruments and archived for future analysis. Nylon filters and a portion of each quartz filter undergoes destructive analysis and a remaining part of the quartz filters are retained for archive.

Over the period covered in this study, two different TOR instruments were employed to measure OC, EC and TC. Quartz filters sampled prior to 2016 where analyzed on a DRI Model 2001 thermal optical carbon analyzers (Chow et al., 1993) while filters collected beginning in January of 2016 were analyzed on a DRI Model 2015 multi-wavelength thermal optical carbon instrument (Magee Scientific – Berkley, USA)(Chow et al., 2015). Both instruments use the IMPROVE_A protocol (Chow et al., 2007b), which outlines the temperature step, gaseous environment in the instrument and that reflectance is used to define the split point between OC and EC. To correct for gas phase adsorption onto the quartz filter, the monthly median field blank OC concentration is subtracted from each OC measurement during that sample month. Carbon concentrations are reported in $\mu g/m^3$.

An in house Hybrid Integrating Plate and Sphere (HIPS) system evaluates light absorption from the PTFE filters in the IMPROVE network (White et al., 2016). In this work, the measured absorption coefficient (*Fabs*) is converted into a TOR EC equivalent concentration assuming a Fabs / EC ratio of 10 m^2g^{-1} (Malm et al., 1994). The resulting value, referred to as HIPS Black Carbon (HIPS BC), is used as part of a quality control procedure to evaluate potential outliers in TOR EC measurements.

Data from gravimetry and X-ray fluorescence (XRF) analysis obtained from PTFE filters and ion chromatography from the nylon filters are also used in this study. Additional information on routine IMPROVE methods can be found on the IMPROVE website (http://vista.cira.colostate.edu/Improve/). IMPROVE data are available online at (http://views.cira.colostate.edu/fed).

https://doi.org/10.5194/amt-2021-382
Preprint. Discussion started: 3 December 2021


Atmospheric Measurement Techniques Discussions

2.2 Outlier removal

Data were screened for outliers to eliminate their influence on the results. Out of the ~61,500 total number of samples in the three-year period, fewer than 800 were excluded from the analysis due sampling issues or missing TOR, XRF or IC data. In addition, 65 samples collected at the Wheeler Peak Wilderness (New Mexico) site between November 2015 and April 2016 were excluded due to an EC contamination caused by a diesel-powered ski lift.

Potential outliers in TOR measurements were investigated by regressing TOR EC against HIPS BC concentrations. Samples with differences exceeding a predefined threshold value (0.68 $\mu g/m^3$) were flagged as potential outliers (section S2). The status of these samples was confirmed by building separate TOR EC and HIPS BC calibrations. The poor agreement between TOR EC and FT-IR EC concentrations contrasts with the nearly 1:1 relationship HIPS BC and FT-IR BC predicted values indicating that TOR EC concentrations were likely compromised (Section S2). For the period considered in this study, 112 samples with faulty TOR EC values were identified and excluded from further analysis. The number of valid sample spectra retained in this study is 61,462.

2.3 Fourier-transform infrared (FT-IR) analyses

Since 2015, all PTFE in the IMPROVE network have been analyzed by infrared spectroscopy for research and evaluation purposes. FT-IR measurement occurs after gravimetric analysis and prior to XRF and HIPS to prevent possible loss of volatile species under the mild vacuum in XRF. Three FT-IR spectrometers including one Tensor 27 and two Tensor 2 instruments (Bruker Optics, Billerica, MA) equipped with a pre-aligned mid-IR source and a liquid nitrogen-cooled wide-band mercury cadmium telluride (MCT) detector were used for spectra acquisition in the range 4000 - 420 cm^{-1} by averaging 512 scans at a nominal resolution of 4 cm^{-1}. The single beam signal associated with each PTFE filter was converted to an absorbance spectrum using the most recent zero reference signal, updated hourly.

Previously, it was determined that calibration transfer between multiple FT-IR instruments is not required as long as their spectral response is carefully matched by controlling a set of key environmental and instrumental parameters (Debus et al., 2019). Briefly, each mercury cadmium telluride (MCT) detector is connected to an automatic liquid nitrogen micro dosing system (NORHOF, Ede, Netherlands) designed to improve signal stability and maintain a high signal to noise ratio. The repeatability and reproducibility of the filter position relative to the IR beam is controlled via a house-built sample chamber (4.0 × 5.1 × 4.5 cm) mounted inside the instrument sample compartment. Details regarding the chamber design have been published elsewhere (Debus et al., 2019). Finally, the contribution of water vapor and carbon dioxide to the signal was minimized by continuously purging both the sample chamber and the optical bench with a VCD Series CO_2 adsorber / dryer system (PureGas LLC, Broomfield, CO). For each sample, the acquisition procedure involves a 4 minutes purge period followed by a spectrum collection lasting

https://doi.org/10.5194/amt-2021-382
Preprint. Discussion started: 3 December 2021


Atmospheric Measurement Techniques Discussions

about 1 minute. An in-house macro interfaced to the OPUS software (Bruker Optics, Billerica, MA) controls each step. PTFE filters were measured in transmission mode without sample preparation. No interpolated data (from zero-filling) are included in the final raw spectra. Collected spectra are subjected to weekly quality control procedures detailed in (Debus et al., 2019). Duplicate and replicate measurements were also performed to evaluate instrument stability and found to be within +/- 10%.

2.4 Multivariate Calibration Model - Partial Least Squares (PLS) Regression

While the presence of certain category of atmospheric compounds can be identified qualitatively from an FT-IR spectrum, an accurate quantification of their concentration requires calibration. PLS is a commonly used algorithm to relate a multi-wavenumber measurement to any particular sample properties such as concentration (Wold et al., 2001). In brief, PLS maximizes the co-variance between a set of response variables (species measurements) and a reference measurement (FT-IR spectra) from which equivalent predicted values are desired. In so doing, the optimal combination of response variables best describing the reference measurement is identified and the selected features are used to build a multivariate calibration. With all least-squares calibration methodologies, concentration-dependent biases in residuals that are determined by the quality of fit (R^2) and dynamic range of the data are expected due to the nature of least-squares estimation (Besalú et al., 2006; Draper and Smith, 1998, pp. 63-64,173,638). For further discussion of these biases, see Section S1.

The applicability of PLS to quantify carbonaceous aerosol species (Reggente et al., 2016; Weakley et al., 2016, 2018a) or functional groups (Boris et al., 2019; Ruthenburg et al., 2014) collected on PTFE filters in various monitoring networks and field campaigns has been successfully demonstrated. A complete review of the implementation of PLSR calibration in the framework of atmospheric particulate matter characterization has been recently published (Takahama et al., 2019).

To evaluate model performance, FT-IR predicted concentrations were regressed against their reference measurement to quantify residuals and a series of metrics. Reported figures of merit include the coefficient of determination (R^2), bias, error and the method detection limit (MDL). Residuals are defined as the difference between predicted and reference concentrations, bias corresponds to the median residual while error is the median absolute residual. To facilitate inter-model comparison, relative performance metrics were calculated by normalizing the values by their reference value. FT-IR PLSR calibration MDL was estimated from field blank predicted concentrations as the 95th percentile minus the median residuals, as is done for other species in the IMPROVE network http://vista.cira.colostate.edu/improve/wp-content/uploads/2021/07/IMPROVE-SOP-351_Data-Processing-and-Validation_2021_final.pdf. Performance is reported for all samples together regardless if the samples were included in the calibration. This enables comparison between models with different samples used for calibration.

https://doi.org/10.5194/amt-2021-382
Preprint. Discussion started: 3 December 2021


Atmospheric Measurement Techniques Discussions

For further insight into model prediction accuracy, the distribution in FT-IR residuals is qualitatively compared with residuals from collocated measurements. Collocated quartz filters are collected at the Everglades (FL), Hercules-Glades (MO), Medicine Lake (MT) and Phoenix (AZ) sites. Similarly, collocated Teflon filters are sampled at Mesa Verde (CO), Proctor Maple Research Facility (VT), Saint Marks National Wildlife Refuge (FL), Yosemite (CA) and Phoenix (AZ) sites while collocated nylon filters are featured at the Phoenix (AZ), Frostburg Reservoir (MD), Mammoth Cave (KY) and San Gabriel (CA) sites.

Data handling and analysis was performed in Matlab R2018a (The MatWorks, Inc, Natick, MA, United States) using the statistics and signal processing toolboxes. PLS was computed via the libPLS Matlab package (v1.9) (Li et al., 2018).

2.5 FT-IR Calibrations for Predicting PM Composition

This section presents the design of calibrations for quantifying the concentration of major atmospheric species by taking advantage of the composition-based information embedded within an FT-IR spectrum. In practice, spectra are calibrated against reference measurements from TOR, XRF, IC, HIPS and gravimetric analysis with the aim of predicting concentrations of atmospheric constituents using only spectra of PTFE filters as input.

A multilevel model (Snijders and Bosker, 2011; Takahama et al., 2019) is proposed in which dedicated calibration models for subgroups of samples are constructed, and applied according to a predetermined selection criterion for each sample. This model considers two subgroups: i) samples determined to be dominated by biomass burning, which are calibrated with similar samples, and ii) the remaining samples, which are calibrated with samples from a limited number of sites. To establish baseline performance metrics for comparison, a “Global model” in which a single calibration (for each species) is constructed from all samples considered together and described in Section S1 (Supplement).

The first step in the development of the Multilevel model consists of screening for biomass burning samples. These samples are removed from consideration during the site selection process. A simple detection method combining estimates of key functional group spectral peak areas and spectral dissimilarity metrics were used to segregate biomass burning samples from all other samples. Next, a Gaussian Mixture Model (GMM) was applied to the spectra of all non-biomass burning samples. The GMM exploits the specificity of the infrared signal for organic and inorganic species. The GMM was implemented with the aim of clustering the non-biomass burning FT-IR spectra into groups sharing similar spectral features (Section 2.5.2). Those groups were later used as part of the methodology for selecting sites with representative atmospheric composition. Spectra from the year 2015 were used as a benchmark to validate the biomass burning detection strategy, build the GMM and establish the list of representative sites where

https://doi.org/10.5194/amt-2021-382
Preprint. Discussion started: 3 December 2021


Atmospheric Measurement Techniques Discussions

multi-filter collection/multi-analyses should be retained (section 2.5.2). The identified biomass burning samples are used to build a calibration for biomass burning samples (Section 2.5.1).

2.5.1 Biomass burning model

FT-IR spectra were used to estimate functional group areas and calculate spectral dissimilarities metrics to segregate biomass burning samples from all other samples. Although this paper focuses on using FT-IR to measure the major aerosol components in routine speciated aerosol monitoring networks, FT-IR is more frequently used to measure organic functional groups (e.g. (Russell et al., 2011; Ruthenburg et al., 2014; Boris et al., 2019). Specific regions in the IR spectra correspond to specific functional groups. Peak areas, calculated from baseline corrected spectra (see Section S3 for baseline procedure), for carbonyl, OH and CH were used rather than functional group calibrations for simplicity. Because the relative functional group peak area tends to increase significantly as the cumulative peak area decreases, typically for low mass deposition samples, an estimate of spectral dissimilarities, the squared Mahalanobis distance (D_i^2), for each site is also considered to minimize false detection. The Mahalanobis distance (Mahalanobis, 1936; Cios et al., 1998) is a measure of the spectral dissimilarity between a given spectrum at a site and the mean spectrum at the site. Taking advantage of D_i^2 and relative functional group areas, a set of criteria were established from observations at known wildfire sites during wildfire season (O'Dell et al., 2019). First, samples collected under heavy smoke conditions whose spectra fulfill C–H ≥ 2 %, C=O ≥ 15 % and $D_i^2 \geq 3\,\overline{D^2}$ were detected (Section S3). This group of spectra tend to have large D_i^2 values and, consequently, the $3\,\overline{D^2}$ threshold often excludes samples with low to moderate biomass burning contributions. For a more inclusive detection, spectra from the first group were removed from consideration, the D_i^2 values are updated for each sample and the plots were regenerated. The cut-off value for the relative carbonyl functional group area was lowered to 8 % while other parameters were not changed. Spectra identified by the first and second rounds are considered biomass burning samples. This procedure is performed for each site and for each year of sample collection (Section S.3)

Recent work has shown that smoke samples may be identified using techniques such as cluster analysis and labeling (Burki et al., 2020) similar to the GMM used here and through detection of molecular markers – levoglucosan and lignin – or peak profiles in FT-IR spectra (Yazdani et al., 2021a, b). For the large data set in this work (~20,000 samples in 2015), cluster analysis resulted in multiple clusters that could be associated with smoke-impacted samples likely due to the variations in fuel, oxidation conditions, and contributions from other sources. Therefore, for this work we selected a single group of smoke-impacted samples based on specific organic features known to be present in FT-IR spectra. While the criteria for smoke-impact labeling can be defined differently according to each intended purpose, the method presented here is demonstrated to sufficiently partition the samples for building accurate submodels to predict concentrations of PM constituents.

https://doi.org/10.5194/amt-2021-382
Preprint. Discussion started: 3 December 2021


Atmospheric Measurement Techniques Discussions

While ions and crustal species are not necessary correlated with wildfire emissions, the Biomass Burning sub-model for accounts for interferences that are necessary to track in order to maintain high prediction accuracy for samples collected on smoky days.

2.5.2 Limited Sites Model

To assess major $PM_{2.5}$ composition regimes in the network and to identify representative sites to use as calibration standards in the Limited Sites model, screening of all FT-IR spectra (except samples identified as biomass burning samples) across all locations and seasons was performed by building a Gaussian Mixture Model (GMM) (Bilmes, J. A., 1998; Hastie, T et al., 2009). The basic idea behind GMM is to group FT-IR spectra into clusters of similar spectral shape using a probabilistic approach describing the likelihood that any given spectrum belongs to a particular class. To minimize the concentration dependence and emphasize composition, raw spectra were transformed to second derivative spectra using a 2^{nd} order, 21 point, Savitzky-Golay filter (Savitzky and Golay, 1964), differenced with filter blank spectra and divided by their respective Euclidean norm (Bro and Smilde, 2003). Additional details about the GMM pre-processing and implementation as well as cluster interpretation are provided in Section S4.

After classification, a single site per cluster was selected to represent the atmospheric composition captured in that cluster. For any given cluster, the retained location was defined as the site with the largest number of classified spectra with the highest probabilities of belonging to that cluster. To prevent misleading site selection and enhance spatial coverage, the following set of decision rules were used: *i)* if the same site is representative of two clusters, it is ascribed to the cluster with the largest number of classified spectra from that site, *ii)* if none of the retained sites accounts for a given spatial region or known source type in the network, an additional site with the highest number of classified spectra is selected from a nearby cluster, and *iii)* only sites under continuous operation between 2015 and 2017 are eligible for selection. Criteria *ii)* was invoked once to add a site in the Midwest to improve spatial coverage in that region and to capture prescribed fire emissions in Kansas. All non-biomass burning samples from selected sites were used as FT-IR calibration standards for all species and all non-biomass burning samples are predicted with these models. Once established, the selected sites are not re-evaluated but instead were used in all subsequent years as would occur in practice.

2.5.3 Application of Multilevel Model

Multilevel model is the combined FT-IR predicted concentrations from the Limited sites and Biomass burning models. Multilevel modeling will be discussed in the context of carbonaceous aerosols before extending the modeling to other atmospheric constituents with detectable infrared signatures. In addition to OC and EC, species evaluated for FT-IR prediction include $PM_{2.5}$ mass, soil elements (silica, aluminum, calcium, titanium, iron), anions (sulfate, nitrate) and HIPS BC. Next, the years 2016 and 2017 will be examined to assess the long-term stability of the

https://doi.org/10.5194/amt-2021-382
Preprint. Discussion started: 3 December 2021


Atmospheric Measurement Techniques Discussions

proposed Multilevel strategy by screening for smoke samples and re-calibrating each year using the sites selected using 2015 data.

3 Results and discussion

In the following sections, the quality of FT-IR based calibrations for quantifying aerosol composition across continental US and their long-term applicability to large speciation monitoring networks will be assessed. Section 3.1 describes the selected calibration samples for the Biomass Burning and Limited Sites models. In Section 3.2, Biomass Burning and Limited model performance will be briefly reviewed before exploring the Multilevel FT-IR predictions for all samples. Initially focused on carbonaceous species on PTFE samples collected in 2015, FT-IR predictions will be extended to other atmospheric constituents and years.

3.1 Multilevel modeling – Calibration sample selection

3.1.1 Biomass burning sample selection

Using the methods described above, 492 samples impacted by biomass burning emissions were identified in 2015 (2.5 % of the network), 288 samples in 2016 (1.5 %), and 817 samples in 2017 (3.7 %). The mean OC concentration of the biomass burning samples range was 5.6 – 8.3 $\mu g/m^3$ with maximum concentrations extending from 44.5 to 97 $\mu g/m^3$ over the three year period. Similarly, per year, the mean EC concentration varies between 0.61 – 0.9 $\mu g/m^3$ with maximums up to 2.9 – 3.9 $\mu g/m^3$. Mean OC/EC ratios are larger than 7, in agreement with past literature (Schichtel et al., 2008; Sorooshian et al., 2011). Analysis of the detected samples shows reliable spatial and seasonal distributions, consistent with biomass burning emissions predominantly in summer and fall across the Pacific North West and Northwestern US (Section S3). Two-thirds of the identified samples were selected (Section S5) as calibration standards for the calibration and resulting model was applied to the remaining third of the smoke impacted samples.

3.1.2 Limited Sites model – clusters and retained sites

Figure 1 shows the spatial distribution of the 21 sites selected for Limited sites model. From a spatial standpoint, retained sites appear reasonably scattered across the network including Hawaii and the Virgin Islands. Clusters are represented by a distribution of urban and rural sites. One urban cluster is represented by Fresno and contains mostly urban samples from Fresno and Phoenix. All other clusters contain mostly rural and pristine sites. However, two other urban sites were retained, Phoenix and Birmingham. The Phoenix cluster contains samples from the southwest in the spring. The Birmingham site along with the Tallgrass site represent a non-western cluster in the spring and summer.

https://doi.org/10.5194/amt-2021-382
Preprint. Discussion started: 3 December 2021

Atmospheric Measurement Techniques Discussions

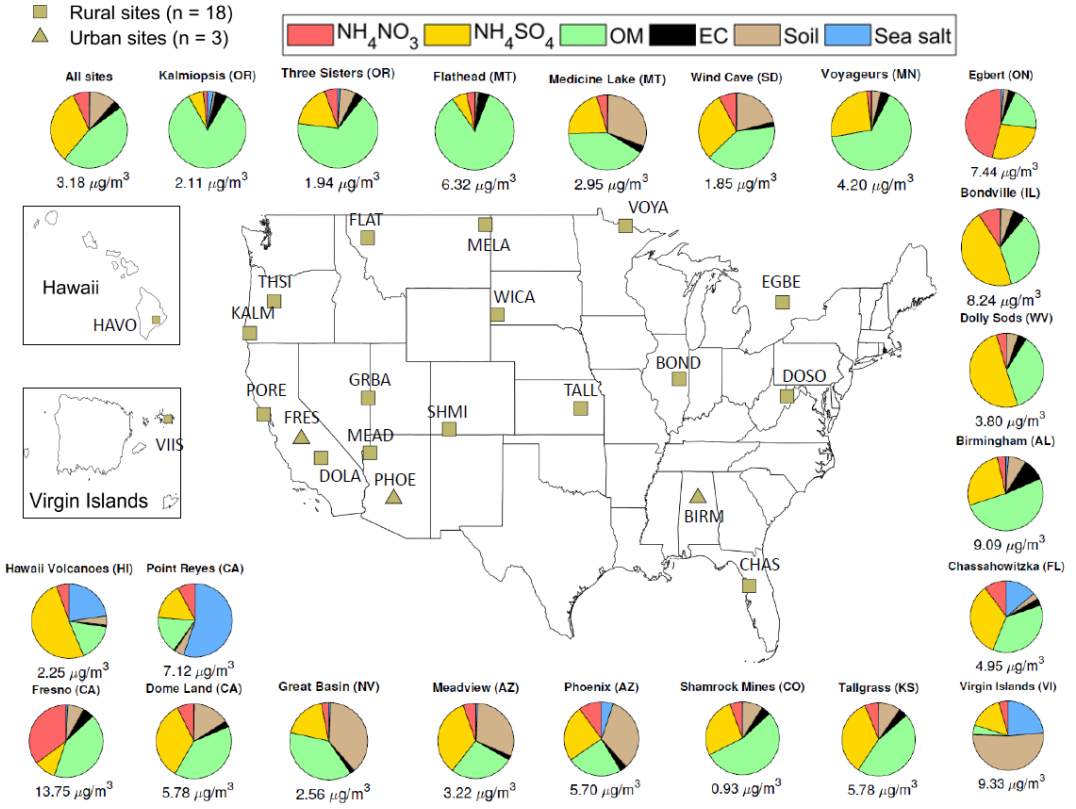

Figure 1: Spatial distribution, median $PM_{2.5}$ concentration and composition of the 21 representative sites. Sites are identified by the four letter site code which is the first four letters of a single word site name (Fresno = FRES) or the first two letters of the first and second word for two word site names (Dome Land = DOLA. The composition is obtained from IMPROVE measurements and the IMPROVE reconstructed fine mass equation. The top left pie chart representing the median $PM_{2.5}$ composition across all sites and samples is given for comparison.

The clusters are also seasonally distributed (Section S6): five clusters are dominated by fall - winter samples, ten clusters containing summer samples (along with varying number of spring and fall samples), two clusters are predominately spring and one is spring - fall. Three clusters have little seasonality.

Because FT-IR spectra are clustered based on composition, the first step in assessing the representativeness of the 21 sites is to compare the concentration ranges. For this purpose,

https://doi.org/10.5194/amt-2021-382
Preprint. Discussion started: 3 December 2021

Atmospheric Measurement Techniques Discussions

distributions in TOR OC and EC concentrations excluding biomass burning samples are compared for the 21 sites used for calibration and the 140 remaining sites. In Fig. 2, the two probability density functions are very similar for both OC and EC despite large differences in sample populations (2572 and 16,543, respectively). In addition to matching the range of carbonaceous concentrations observed in the rest of the network, the presence of species interfering with organic functional groups should also be accounted for by the calibration. Because ammonium absorptions overlap with carbonaceous absorptions, situations where ammonium to OC and ammonium to EC ratios are different between calibration samples and samples to be predicted were associated with additional sources of bias and error (Dillner and Takahama, 2015a, b). Although not measured in IMPROVE, ammonium concentration is approximated from nitrate and sulfate assuming both species are fully neutralized. The corresponding probability distribution in Fig. 2 confirms the equivalence between the ranges of ammonium/OC and ammonium/EC concentrations spanned by the Limited sites samples and the overall network. In section S6, Fig. S6-3 shows reasonable agreement between the selected sites and the rest of the network for PM2.5 mass, ions, elements and HIPS BC. Together, these results suggest the list of 21 sites is a suitable representation of network variations in OC and EC and their relative proportion to ammonium, and for all other predicted constituents.

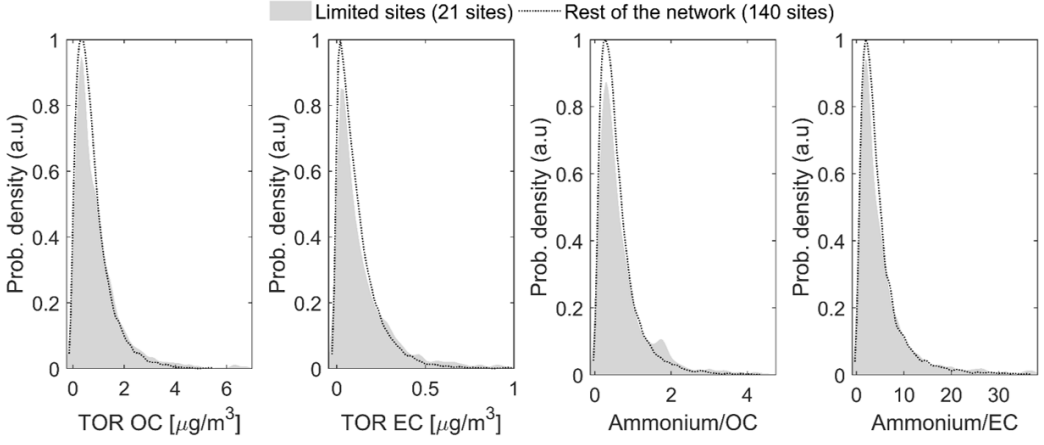

Figure 2: Comparison of probability density function for OC, EC and ammonium concentrations in 2015 between the 21 sites retained for Limited calibration and the rest of the network.

The spatial and seasonal as well as the urban and rural diversity supports the compositional diversity of the selected sites as shown in Fig. 1. The three urban sites have distinct characteristics. At the Fresno, CA site, the composition is dominated by nitrate (35 %) and organic matter (42 %) with an autumn – winter pattern consistent with agriculture and residential wood burning activities (Ngo et al., 2010) as well as with the formation of secondary aerosols during

https://doi.org/10.5194/amt-2021-382
Preprint. Discussion started: 3 December 2021


Atmospheric Measurement Techniques Discussions

stagnation events and a low inversion layer (Watson and Chow, 2002). Phoenix, AZ site features a strong soil component (33%) associated with spring dust storms and windblown dust and equal proportions of ammonium sulfate (25 %) and OM (24 %) occurring mostly in spring and summer. The ammonium sulfate and organic matter has been attributed to regional power production and traffic (Brown et al. 2007). In contrast, Birmingham samples show little seasonal trend with elevated OM (52 %) and EC (10 %) fractions originating from various combustion processes including vehicle exhaust, biomass burning and biogenic secondary organic aerosols (Blanchard et al. 2016). The other dominant species at this site is ammonium sulfate (26 %), characteristic of coal burning and industrial activities in the East (Watson et al. 2015).

Among rural sites, four noticeable patterns in $PM_{2.5}$ composition are distinguishable. The first corresponds to OM fractions accounting for more than two-thirds of the filter mass. High OM samples are encountered at four locations in Northwestern US, namely the Kalmiopsis (OR), Three Sisters (OR), Flathead (MT) and Voyageurs (MT) sites. Samples from Voyageurs (MN) and Flathead (MT) sites are from Summer-Fall and present elevated median $PM_{2.5}$ concentrations (4.20 $\mu g/m^3$ and 6.32 $\mu g/m^3$, respectively) and very large percentage of OM consistent with biomass burning emissions. Kalmiopsis (OR) and Three Sisters (OR) samples have a lower and nearly identical median $PM_{2.5}$ concentration (≈ 2 $\mu g/m^3$) but differ in their monthly distribution with the former displaying more winter samples than any other season whereas the later shows little seasonality.

The second type of sites have high OM and sulfate concentrations. Both Shamrock Mines (CO) and Tallgrass Prairie (KS) sites have larger OM than sulfate content. However, the Colorado site has more autumn – winter samples, represents samples in the Rockies and Alaska and an overall small median $PM_{2.5}$ concentration (< 1 $\mu g/m^3$). The Kansas site has a majority of spring samples, representing non-western samples and has a significantly larger $PM_{2.5}$ concentration (≈ 6 $\mu g/m^3$) that is attributed to prescribed burning near the Tallgrass site (Whitehill et al. 2019). Other sites have higher median sulfate concentrations (~50%) than OM concentrations (~40%) such as Dolly Sods (WV) and Bondville (IL). The monthly sample distribution indicates seasonal influences: Bondville (IL) samples are mostly from the summer and the concentrations are relatively high while the Dolly Sods (WV) site samples are mostly not in the summer with lower concentrations. Because the spectra were normalized to minimize influence of concentration, these two clusters likely have different organic composition even though the relative amount of OM is the same. Finally, situations where sulfate and OM are present in equal proportions (≈ 36 %) are reported at the Dome Land (CA) and Chassahowitzka (FL) pristine sites mainly featuring spring – summer and winter samples, respectively.

A third group of noteworthy $PM_{2.5}$ compositions at rural sites contain a large fraction of (> 20 % of the total mass). The Virgin Islands (VI) site presents the highest soil fraction across the network 52 % of the total $PM_{2.5}$ mass, mostly originating from long-range Sahara soil dust transport

https://doi.org/10.5194/amt-2021-382
Preprint. Discussion started: 3 December 2021


Atmospheric Measurement Techniques Discussions

(Holmes and Miller 2004). In addition to sulfate and OM, elevated soil contributions are observed for the Wind Cave (SD), Meadview (AZ), Medicine Lake (MT), and Great Basin (NV) sites with soil content between 20 and 40%. Although the seasonality is somewhat different between these sites, they all have many samples from the spring suggesting the dust is due at least in part to spring dust storms and may also contain resuspended road dust and more localized dust sources.

A fourth and final distinct category of $PM_{2.5}$ composition includes a collection of sites with unique local atmospheric pollution sources, specific to those locations. The Hawaii Volcanoes (HI) site where sulfur emitted as part as the volcanic activity, contains 51% sulfate along with sea salt (23 %). Another location with unique composition is the Point Reyes (CA) site where the sea salt contribution reaches 55% of the median filter mass for the clustered samples, larger than any other marine site in the network. Finally, the Egbert (ON) Canadian site, representing the upper Midwest in winter is dominated by nitrate (46 %), sulfate (27 %) and OM (20 %).

As described above, the 21 sites retained for the Limited sites sub-calibration present seasonal, regional and compositional features consistent with known or expected trends in $PM_{2.5}$ across the network. The median $PM_{2.5}$ mass at those locations covers a broad range of concentrations ranging from 0.93 $\mu g/m^3$ to 13.75 $\mu g/m^3$ and includes both urban and rural sites. Capturing the large variability in $PM_{2.5}$ composition and concentration is essential to ensure the proposed site list is a representative subset of the parent network. However, it should be mentioned that the proposed site list is not unique but is one of the many feasible solutions since sites whose samples clustered together in the GMM are likely inter-exchangeable.

3.2 Evaluation of Biomass Burning Model

Prior to describing the overall results from the Multilevel model, the Biomass Burning model is evaluated to determine if the biomass burning model improves predictions for those samples. To evaluate the quality of the biomass burning model, the predictions are compared to a global model (section S1) which contains a few samples from all 160 sites which are mostly non-smoke samples but does contain a few smoke samples. Visual inspection of Fig. 3 suggests the equivalence of the biomass burning models to the global model at the lower end of the concentration range. However, improvement in prediction accuracy can be claimed at high concentrations for the Biomass Burning model. The gain in model performance is subtle for OC and TC; however, for EC, predictions benefit from having a dedicated calibration for samples impacted by wildfire emissions, with an increase in R^2 from 0.747 to 0.902 (Section S7).

https://doi.org/10.5194/amt-2021-382
Preprint. Discussion started: 3 December 2021

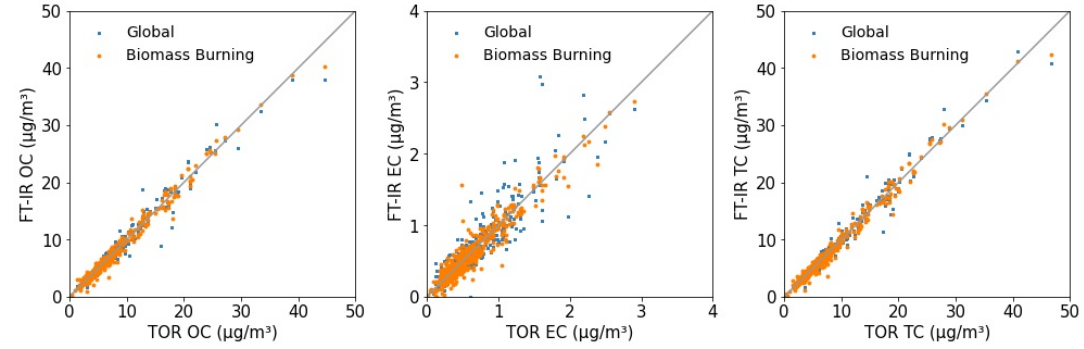

Figure 3: Inter-model OC (left), EC (middle), TC (right) comparison between global (section S1) and Biomass Burning predicted concentrations for the 492 samples classified as biomass burning in 2015. EC prediction, in particular, benefit from having a dedicated Biomass Burning calibration model.

Therefore, we retain the biomass burning model as part of the multilevel model and present the results for the Multilevel model below.

3.3 Multilevel modeling – Performance evaluation

3.3.1 Carbonaceous aerosol predictions

Figure 4 shows the correspondence between FT-IR Multilevel concentrations for OC and EC and TOR measurements for 2015 (plot for TC can be found in Section S9) and Table 1 lists the prediction metrics for all 3 carbonaceous components. The visual agreement between FT-IR and the reference measurements of OC and EC is high but EC shows higher scatter than the other measurements. Table 1 indicates that FT-IR OC and TC has higher prediction quality than EC but both perform satisfactorily. FT-IR OC and TC error is on par with TOR precisions (Table 1) indicating that FT-IR does not add significant additional error to the measurement. FT-IR EC predictions, however, have higher error than TOR precision. With respect to reference (TOR) measurements, concentration-dependent biases in residuals that are determined by the quality of fit (R^2) and dynamic range of the data are expected due to the nature of least-squares estimation (Besalú et al., 2006; Draper and Smith, 1998). For bias defined as FT-IR predictions minus the reference (TOR) measurement, least-squares estimator causes an apparent linear bias which is positive at the low end of the concentration range and negative at the high end of the concentration range. (see Section S8 for further discussion). The satisfactory agreement between FT-IR and TOR concentrations as well as the equivalence agreements using the global model (Section S1) support the validity of the proposed Multilevel modeling in the context of carbonaceous aerosols prediction from PTFE filters in large speciation networks.

https://doi.org/10.5194/amt-2021-382
Preprint. Discussion started: 3 December 2021

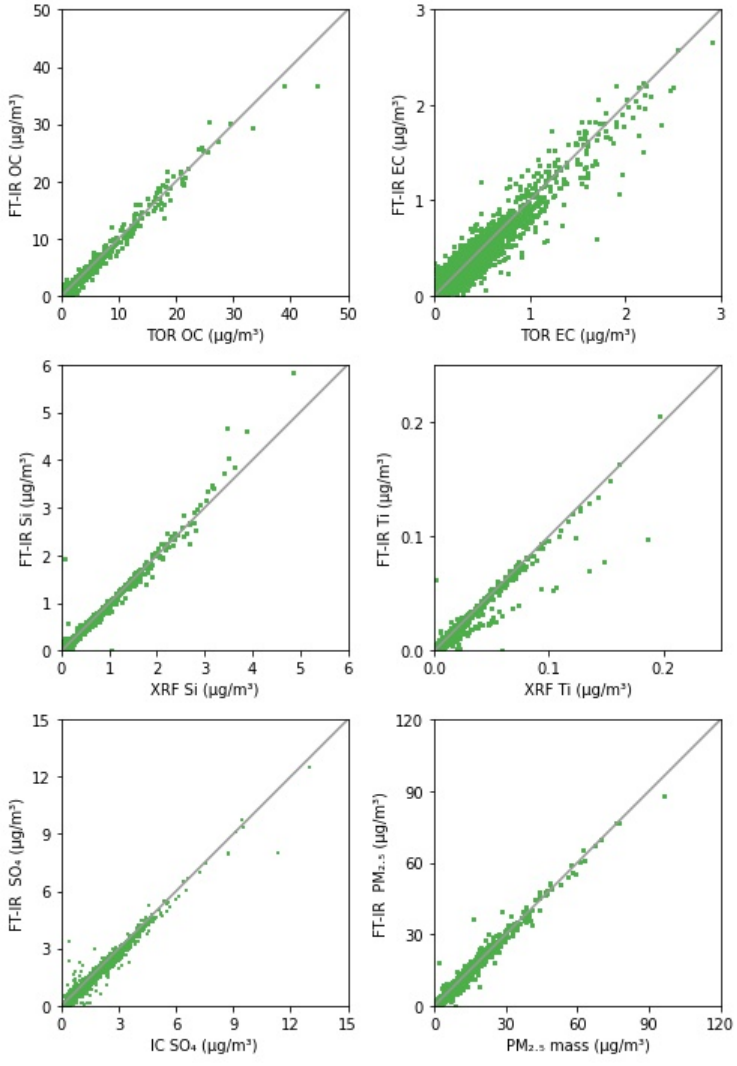

Figure 4: Comparison of predicted FT-IR OC, EC, Si, Ti, SO_4 and mass concentrations using the Multilevel model against their reference measurements. Each subplot contains all 19,608 samples collected in the year 2015.

Table 1: Summary of Multilevel model performance for IR-active atmospheric constituents for 19,608 spectra analyzed by FT-IR in the year 2015.

https://doi.org/10.5194/amt-2021-382
Preprint. Discussion started: 3 December 2021

Atmospheric Measurement Techniques Discussions

Species	R^2	Bias [µg/m³]	Bias (%)	Error [µg/m³]	Error (%)	Reference Data Error[1] (%)	MDL [µg/m³]	< MDL (%)
OC	0.983	0.01	1.6	0.08	12	10	0.06	0.9
EC	0.912	0	1.7	0.02	30	15	0.04	20.7
TC	0.984	0.01	1.2	0.08	12	11	0.07	1.3
BC	0.92	0	-0.3	0.03	23	---	0.04	19.3
Si	0.983	0	2.2	0.01	11	13	0.01	9.7
Al	0.985	0	2.2	0	12	10	0	4.7
Ca	0.979	0	1.1	0	13	9	0	6.9
Ti	0.941	0	2.7	0	21	16	0	14.9
Fe	0.95	0	1.1	0	25	8	0.01	19
SO_4	0.983	0	0.1	0.03	6	2	0.03	0.9
NO_3	0.927	0.02	15.3	0.07	54	8	0.07	21.8
$PM_{2.5}$ Mass	0.985	0.03	1	0.18	6	6	0.25	1.1

[1]Median relative error for TOR, XRF, IC and gravimetric analysis. OC, EC and TC median relative error estimated from collocated sampling as measurement error/uncertainty is not reported by IMPROVE for this components. For all other components, the normalized error was calculated as the uncertainty divided by the concentration prior to selecting the median. BC is not reported by IMPROVE so measurement error is not estimated.

In addition to OC, EC and TC, light absorption which is predominantly due to black carbon, is also a measure of one fraction of the carbonaceous aerosol. FT-IR calibrations are found to be adequate for replicating HIPS BC measurements (Section S9). As expected, the corresponding model is similar in performance to its EC with R^2 and relative error of 0.920 and 23.3 %, respectively (Table 1). FT-IR BC residuals have a broader interquartile range than in the HIPS BC collocated data (Section S9). We attribute this effect to a difference in signal to noise ratio and sensitivity to chemical interferents between the two analytical techniques. While HIPS exploits the strong absorption properties of refractory carbon in the visible domain, the weak absorptivity of EC in the mid-infrared domain (Niyogi et al., 2006) and the presence of overlapping species makes the quantification less accurate.

3.3.2 Elemental oxide predictions

Taking advantage of known mineral absorbance bands in the mid-infrared range (Hahn et al., 2018; Madejová and Komadel, 2001; Senthil Kumar and Rajkumar, 2013) (Section S9), Multilevel calibrations for soil elements were evaluated for the five crustal elements commonly used to estimate soil: silicon, aluminum, calcium, titanium, and iron (Table 1 and Fig. 4 for Si and Ti). All models present a satisfactory agreement between XRF and FT-IR predicted concentrations (R^2 > 0.94). The quality of prediction of the elemental oxides falls into two groups. The first group

https://doi.org/10.5194/amt-2021-382
Preprint. Discussion started: 3 December 2021


Atmospheric Measurement Techniques Discussions

includes silicon, aluminum and calcium and is characterized by moderate relative errors (11 – 13 %), similar in magnitude to the FT-IR OC model (12 %) and have similar errors to XRF measurements indicating similar to OC and TC that FT-IR does not add additional uncertainty. The second group includes titanium and iron which have larger relative errors (20.9 – 24.8 %), analogous to HIPS BC and EC models (23.3 – 30 %). Comparing residuals to collocated XRF measurements (Section S9) shows that the FT-IR based models have a larger interquartile range. For Fe, XRF uncertainty is quite low and FT-IR adds additional uncertainty to the measurement. XRF Ti measurements have higher error than the other elements but there is an incremental increase in error due to FT-IR. In addition, cross plots of titanium concentrations show a bifurcation (Fig. 4). While most samples fall near their expected titanium concentration, samples collected at the Sycamore Canyon (AZ) site present a systematic negative bias, consistent across years, tentatively attributed to a site-specific soil composition not accounted for by the Limited calibration. Takahama et al. (2019) demonstrated several methods to identify the possible occurrence of anomalous predictions in OC and EC based on comparison of new sample spectra to calibration spectra based on projected PLS scores and regression residual vectors. These samples with systematic negative bias in titanium predictions can presumably be identified using such an approach, provided that compositional differences are detected in the IR spectrum. Although distinct IR fingerprints exist, FT-IR calibrations for quantifying mineral contents should be interpreted with care as specific elements may be indirectly quantified through their correlation with another element even in the absence of clear IR signature (Hahn et al., 2018). For instance, the variable importance in projection (VIP) scores for the Si, Al, and Ti calibrations suggests use of similar spectral variables, with small differences, for prediction of these species (Section S9). However, the 21 GMM sites coverage still meet the necessary requirements for providing a reliable insight into soil composition in the IMPROVE network.

3.3.3 Inorganic ions

The two most abundant inorganic anions quantified in the network: nitrate and sulfate can also be measured by FT-IR (absorption bands used for prediction are discussed in Section S9). FT-IR sulfate concentrations display a satisfactory agreement with the reference IR measurements (Fig. 4). Model performance metrics include R^2 above 0.98 and relative error lower than 10 % as in the FT-IR $PM_{2.5}$ model (Table 1). IC measurements of sulfate are very good have even lower error than FT-IR sulfate. However, FT-IR nitrate concentrations (Section S9) are characterized by a moderate drop in the overall model performance (R^2 = 0.927) while relative bias and error exceed 15 % and 50 %, respectively and the error far exceeds reference IC nitrate measurement error. A direct comparison against differential nitrate concentrations at collocated sites highlights the broad uncertainty in determining nitrate content from PTFE filters (Section S9). Unlike nylon filters for which nitrate is trapped on the surface, nitrate is known to evaporate from PTFE filters. This causes a discrepancy between the mass of nitrate deposited onto the nylon filter and the mass of nitrate on the PTFE filter (Eldred and Ashbaugh, 2004), making FT-IR calibrations with the

https://doi.org/10.5194/amt-2021-382
Preprint. Discussion started: 3 December 2021


Atmospheric Measurement Techniques Discussions

559 nitrate measurements by IC from nylon filters as the reference method error prone. FT-IR based
560 nitrate concentrations, measured in this way, should be considered with caution. A possible
561 alternative is to develop a set of laboratory calibration standards of ammonium nitrate for FT-IR
562 calibration. The nitrate mass on the PTFE would be useful for mass closure exercises on the PTFE
563 filter but would not adequately assess particulate nitrate in the atmosphere.

564 ### 3.3.4 $PM_{2.5}$ mass predictions

565 Since the major aerosol species are shown to be reasonably well measured by FT-IR, it was
566 anticipated that $PM_{2.5}$ mass calibration would perform well. The $PM_{2.5}$ model presents reliable
567 filter mass predictions (R^2 = 0.985) characterized by relative bias and error that are 1/3 to 1/2 of
568 those for OC and on par with gravimetric error (Table 1). The cross plot of gravimetric mass and
569 FT-IR predictions (Fig. 4) shows that $PM_{2.5}$ mass can be accurately predicted across a broad
570 concentration range indicating that FT-IR spectra of PTFE filters do not contain interferents or
571 other limitations that make PM mass predictions error prone.

572 ## 3.4 Long term stability

573 Finally, Multilevel calibrations are extended to 2016 and 2017 to evaluate the inter-year
574 consistency and determine if the assumptions behind Limited Sites and Biomass Burning models
575 remain valid over time. For each sampling year, new calibrations were developed following the
576 framework established for 2015. Models were recalibrated with data from the 21 sites and
577 biomass burning samples were detected by the functional group screening procedure. Fig. 5
578 shows the median relative bias (top) and error (bottom) for the three years of data (cross plots
579 and prediction metrics shown for all predicted species for 2016 and 2017 in Section S10). These
580 results indicate that the modeling methodology provided reasonably consistent results across all
581 three years.

582 Normalized bias for most species is below 3% and normalized error is consistent for all species
583 across all three years. The relative bias for EC and BC are similar to other species in 2015 and
584 2017 but in 2016 they are larger in magnitude than the other two years and different in sign.
585 2016 is the first year of TOR data from the multiwavelength TOR instruments (Chow et al., 2015)
586 so higher bias could be potentially be related the new instruments. However, the HIPS
587 instrument was overhauled beginning in 2017 which provides no explanation for high bias in 2016
588 (http://vista.cira.colostate.edu/improve/Data/QA_QC/Advisory/da0041/da0041_HIPSmodifications.pdf).
589 Further, the EC and BC calibrations are independent of each other except for using
590 the same filters for calibrations (as all species do) so the fact that the median bias is roughly equal
591 but opposite in sign is not due to codependence of the models.

592 In future work, calibrations models will be updated more frequently than annually with the most
593 recent year of ambient samples which may smooth biases and errors due to changes to
594 atmospheric condition and instrument drift.

https://doi.org/10.5194/amt-2021-382
Preprint. Discussion started: 3 December 2021

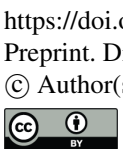

Atmospheric Measurement Techniques Discussions

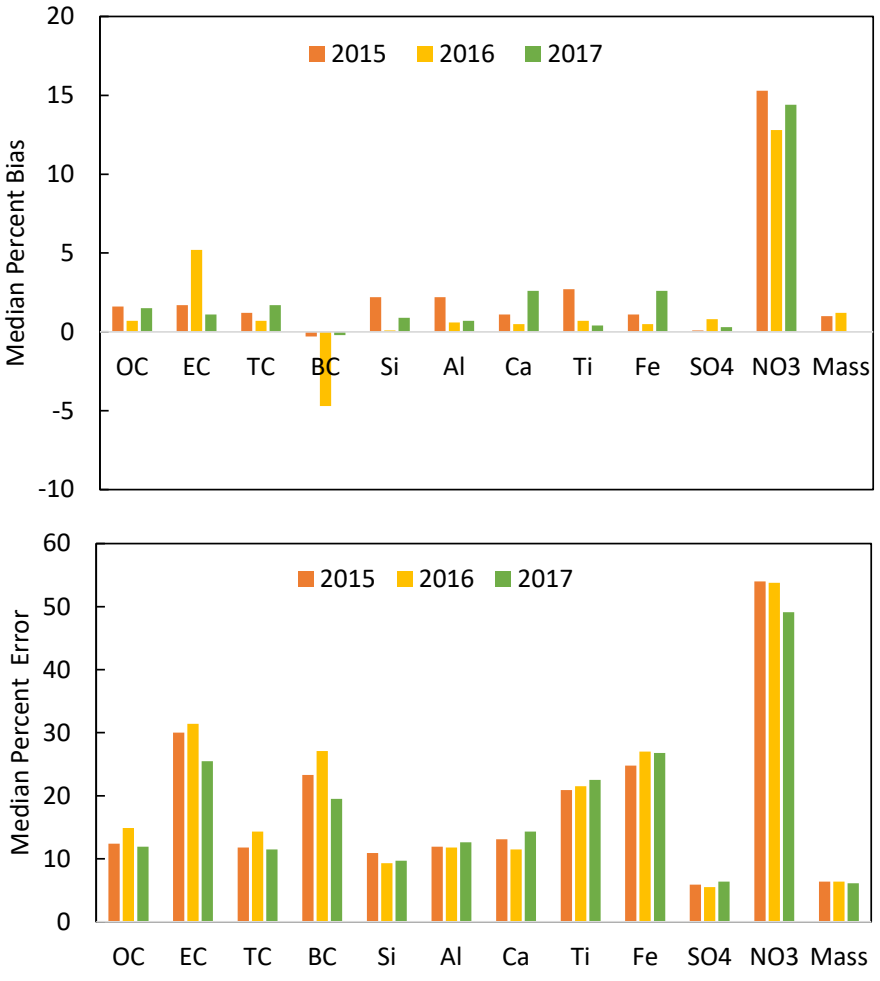

595

596

597 Figure 5. (top) Median Percent Bias and (bottom) Median Percent Error for each constituent
598 measured for each year.

599

600 4 Conclusion

601 In this paper, we investigate the feasibility of an FT-IR method that uses ambient samples as
602 calibration standards and is adapted for use by a large monitoring network. In this method, all

https://doi.org/10.5194/amt-2021-382
Preprint. Discussion started: 3 December 2021


Atmospheric Measurement Techniques Discussions

603 sites in the network collect PTFE filters for FT-IR analysis. A few select sites, used for calibration,
604 would retain all sampling and analyses of current IMPROVE sites to enable re-calibration of the
605 FTIR method on a routine basis. Re-calibration is especially important as atmospheric changes
606 occur and as conditions in the network evolve over time, for example new reference instruments,
607 new or significantly modified FT-IR instruments, changes to sampling protocol or possibly change
608 in filter material. The validity of such a design was evaluated with all PTFE filters collecting $PM_{2.5}$
609 aerosols at 161 IMPROVE sites in 2015 and then tested for all filters in 2016 and 2017.

610 A multi-level modeling algorithm was used whereby smoke impacted samples are identified and
611 predicted by one model and the rest of the samples are predicted by another model developed
612 from 21 selected IMPROVE sites. The data from the two models are combined to evaluate
613 performance of the FT-IR method. The selection of sites was performed such that if one of the
614 21 sites ceases to operate, another site, selected from the same compositional cluster can be
615 used for calibration.

616 The cross-plots and prediction metrics indicate that the Multilevel model is equivalent to
617 conventional calibrations built from samples from every available site. Reliable performance in
618 predicted concentrations were reported for a broad range of atmospheric constituents with
619 detectable infrared signatures such as OC, EC, TC, sulfate, soil elements (Si, Al, Ca, Ti, Fe), light
620 absorption, and $PM_{2.5}$ mass. Due to volatilization off the PTFE filter, nitrate measurements were
621 found to be unsatisfactory. The calibration method was develop using data from 2015, and the
622 same methodology was applied to 2016 and 2017. The model performance metrics in all three
623 years were similar. Results across ~61,500 FT-IR spectra highlight the suitability of the Multilevel
624 calibration design to quantify multiple atmospheric $PM_{2.5}$ species in large monitoring networks.

625 This work presents an alternative, lower cost, filter analysis method to measure speciated aerosol
626 in an operational routine monitoring network. This could be a valuable addition to routine
627 speciated aerosol monitoring networks, such as IMPROVE, by incorporating monitoring sites that
628 collect samples on only a PTFE filter for subsequent analysis. This would provide the opportunity
629 to have a subset of less expensive monitoring site, which could be used for scoping studies to
630 understand the aerosol composition in unmonitored locations. It could also serve as a network
631 cost savings method by having a subset of network sites collect aerosol samples on only a Teflon
632 filter. However, the inability to measure particulate nitrate is a significant deficiency for using
633 this method to replace existing monitoring sites. The FTIR derived aerosol concentrations are
634 also a semi-independent measurement from the routine speciated aerosol measurements.
635 Therefore, routine FTIR measurements would provide valuable QA/QC information for any
636 speciated monitoring network. In addition, FTIR derived concentrations could be used to
637 substitute for missing concentrations in the case where the Teflon sample is valid, but filter
638 samples or analyses on the nylon or quartz fiber filters are not.

https://doi.org/10.5194/amt-2021-382
Preprint. Discussion started: 3 December 2021


Atmospheric Measurement Techniques Discussions

For IMPROVE's urban counterpart, the CSN network, after evaluation of the quality of predictions in CSN, this framework could be used to accomplish goals similar to those of IMPROVE. Additionally, this method could be used to predict samples collected in the Federal Reference Method (FRM) network which is a PM mass only network. Finally, this method, with appropriate ambient standards, could be applied at other regional or international monitoring networks or sites to provide low-cost comprehensive composition data.

https://doi.org/10.5194/amt-2021-382
Preprint. Discussion started: 3 December 2021


Atmospheric Measurement Techniques Discussions

5 Data availability

Data is available at https://doi.org/10.25338/B8TP8V.

6 Author contribution

BD developed the software, performed the formal analysis and visualization for much of the manuscript and wrote the original draft of the manuscript, ATW developed software, performed formal analysis and visualization of the GMM work, ST participated in conceptualization, methodology software, visualization and reviewing and editing the manuscript. KMG developed parts of the biomass burning identification methodology, BS, SC and ASW, provided input throughout the project and reviewed and edited the manuscript , AMD conceptualized of and acquired funding for this project, developed methodology, performed project administration and supervision and reviewed, edited and finalized the manuscript.

7 Acknowledgments

The authors acknowledge funding from the National Park Service in cooperation with the Environmental Protection Agency (P18AC01222). Thanks to Anahita Amiri Farahani for assisting with figures. We are particularly grateful to Kelsey Seibert for overseeing daily FT-IR operations at the University of California Davis and to the numerous undergraduate students who performed spectra collection from 2015 to 2017.

8 References

Besalú, E., Julián-Ortiz, J. V. de., Iglesias, M., and Pogliani, L.: An overlooked property of plot methods, Journal of Mathematical Chemistry, 39, 475–484, https://doi.org/10.1007/s10910-005-9035-z, 2006.

Bilmes, J. A.: A gentle tutorial of the EM algorithm and its application to parameter estimation for Gaussian mixture and hidden Markov models, 4:126, 1998.

Boris, A. J., Takahama, S., Weakley, A. T., Debus, B. M., Fredrickson, C. D., Esparza-Sanchez, M., Burki, C., Reggente, M., Shaw, S. L., Edgerton, E. S., and Dillner, A. M.: Quantifying organic matter and functional groups in particulate matter filter samples from the southeastern United States – Part 1: Methods, Atmos. Meas. Tech., 12, 5391–5415, https://doi.org/10.5194/amt-12-5391-2019, 2019.

Boris, A. J., Takahama, S., Weakley, A. T., Debus, B. M., Shaw, S. L., Edgerton, E. S., Joo, T., Ng, N. L., and Dillner, A. M.: Quantifying organic matter and functional groups in particulate matter filter samples from the southeastern United States - Part 2: Spatiotemporal trends, 14, 4355–4374, https://doi.org/10.5194/amt-14-4355-2021, 2021.

https://doi.org/10.5194/amt-2021-382
Preprint. Discussion started: 3 December 2021

Atmospheric Measurement Techniques Discussions

678 Bro, R. and Smilde, A. K.: Centering and scaling in component analysis, Journal of Chemometrics, 17, 16–
679 33, https://doi.org/10.1002/cem.773, 2003.

680 Burki, C., Reggente, M., Dillner, A. M., Hand, J. L., Shaw, S. L., and Takahama, S.: Analysis of functional
681 groups in atmospheric aerosols by infrared spectroscopy: method development for probabilistic
682 modeling of organic carbon and organic matter concentrations, 13, 1517–1538,
683 https://doi.org/10.5194/amt-13-1517-2020, 2020.

684 Busca, G. and Resini, C.: Vibrational Spectroscopy for the Analysis of Geological and Inorganic Materials,
685 in: Encyclopedia of Analytical Chemistry, John Wiley & Sons, Ltd, 2006.

686 Chow, J. C., Watson, J. G., Pritchett, L. C., Pierson, W. R., Frazier, C. A., and Purcell, R. G.: The dri
687 thermal/optical reflectance carbon analysis system: description, evaluation and applications in U.S. Air
688 quality studies, 27, 1185–1201, https://doi.org/10.1016/0960-1686(93)90245-T, 1993.

689 Chow, J. C., Watson, J. G., Chen, L. W. A., Chang, M. C. O., Robinson, N. F., Trimble, D., and Kohl, S.: The
690 IMPROVE_A Temperature Protocol for Thermal/Optical Carbon Analysis: Maintaining Consistency with a
691 Long-Term Database, 57, 1014–1023, https://doi.org/10.3155/1047-3289.57.9.1014, 2007a.

692 Chow, J. C., Watson, J. G., Chen, L. W. A., Chang, M. C. O., Robinson, N. F., Trimble, D., and Kohl, S.: The
693 IMPROVE_A Temperature Protocol for Thermal/Optical Carbon Analysis: Maintaining Consistency with a
694 Long-Term Database, 57, 1014–1023, https://doi.org/10.3155/1047-3289.57.9.1014, 2007b.

695 Chow, J. C., Wang, X., Sumlin, B. J., Gronstal, S. B., Chen, L.-W. A., Trimble, D. L., Watson, J. G., Kohl, S. D.,
696 Mayorga, S. R., Riggio, G., Hurbain, P. R., Johnson, M., and Zimmermann, R.: Optical Calibration and
697 Equivalence of a Multiwavelength Thermal/Optical Carbon Analyzer, 15, 1145–1159,
698 https://doi.org/10.4209/aaqr.2015.02.0106, 2015.

699 Chukanov, N. V. and Chervonnyi, A. D.: Infrared Spectroscopy of Minerals and Related Compounds,
700 Springer International Publishing, 2016.

701 Cios, K., Pedrycz, W., and Swiniarski, R. W.: Data Mining Methods for Knowledge Discovery, Kluwer
702 Academic Publishers, Norwell, MA, USA, 495 pp., 1998.

703 Corrigan, A. L., Russell, L. M., Takahama, S., Äijälä, M., Ehn, M., Junninen, H., Rinne, J., Petäjä, T.,
704 Kulmala, M., Vogel, A. L., Hoffmann, T., Ebben, C. J., Geiger, F. M., Chhabra, P., Seinfeld, J. H., Worsnop,
705 D. R., Song, W., Auld, J., and Williams, J.: Biogenic and biomass burning organic aerosol in a boreal forest
706 at Hyytiälä, Finland, during HUMPPA-COPEC 2010, 13, 12233–12256, https://doi.org/10.5194/acp-13-
707 12233-2013, 2013.

708 Debus, B., Takahama, S., Weakley, A. T., Seibert, K., and Dillner, A. M.: Long-Term Strategy for Assessing
709 Carbonaceous Particulate Matter Concentrations from Multiple Fourier Transform Infrared (FT-IR)
710 Instruments: Influence of Spectral Dissimilarities on Multivariate Calibration Performance, 73, 271–283,
711 https://doi.org/10.1177/0003702818804574, 2019.

https://doi.org/10.5194/amt-2021-382
Preprint. Discussion started: 3 December 2021

Atmospheric Measurement Techniques Discussions

712 Dillner, A. M. and Takahama, S.: Predicting ambient aerosol thermal-optical reflectance measurements
713 from infrared spectra: Elemental carbon, 8, 4013–4023, https://doi.org/10.5194/amt-8-4013-2015,
714 2015a.

715 Dillner, A. M. and Takahama, S.: Predicting ambient aerosol thermal-optical reflectance (TOR)
716 measurements from infrared spectra: Organic carbon, 8, 1097–1109, https://doi.org/10.5194/amt-8-
717 1097-2015, 2015b.

718 Draper, N. R. and Smith, H.: Applied Regression Analysis, 1998.

719 Eldred, Robert. and Ashbaugh, L. L.: Loss of particle nitrate from Teflon sampling filters: Effects on
720 measured gravimetric mass in California and in the IMPROVE network, 54, 93–104,
721 https://doi.org/10.1080/10473289.2004.10470878, 2004.

722 Friedel, R. A. and Carlson, G. L.: Infrared spectra of ground graphite, 75, 1149–1151,
723 https://doi.org/10.1021/j100678a021, 1971.

724 Hahn, A., Vogel, H., Andó, S., Garzanti, E., Kuhn, G., Lantzsch, H., Schüürman, J., Vogt, C., and Zabel, M.:
725 Using Fourier transform infrared spectroscopy to determine mineral phases in sediments, Sedimentary
726 Geology, 375, 27–35, https://doi.org/10.1016/j.sedgeo.2018.03.010, 2018.

727 Hastie, T, Tibshirani, R, and Friedman, J: The Elements of Statistical Learning: Data Mining, Inference,
728 and Prediction, Second Edition, Springer New York, New York, NY, 2009.

729 Hawkins, L. N., Russell, L. M., Covert, D. S., Quinn, P. K., and Bates, T. S.: Carboxylic acids, sulfates, and
730 organosulfates in processed continental organic aerosol over the southeast Pacific Ocean during
731 VOCALS-REx 2008, 115, https://doi.org/10.1029/2009jd013276, 2010.

732 Hyslop, N. P., Trzepla, K., and White, W. H.: Reanalysis of Archived IMPROVE PM2.5 Samples Previously
733 Analyzed over a 15-Year Period, Environ. Sci. Technol., 46, 10106, 2012.

734 Hyslop, N. P., Trzepla, K., and White, W. H.: Assessing the Suitability of Historical PM2.5 Element
735 Measurements for Trend Analysis, Environ. Sci. Technol., 49, 9247–9255,
736 https://doi.org/10.1021/acs.est.5b01572, 2015.

737 Kuzmiakova, A., Dillner, A. M., and Takahama, S.: An automated baseline correction protocol for infrared
738 spectra of atmospheric aerosols collected on polytetrafluoroethylene (Teflon) filters, 9, 2615–2631,
739 https://doi.org/10.5194/amt-9-2615-2016, 2016.

740 Li, H.-D., Xu, Q.-S., and Liang, Y.-Z.: libPLS: An integrated library for partial least squares regression and
741 linear discriminant analysis, 176, 34–43, https://doi.org/10.1016/j.chemolab.2018.03.003, 2018.

742 Liu, S., Ahlm, L., Day, D. A., Russell, L. M., Zhao, Y., Gentner, D. R., Weber, R. J., Goldstein, A. H., Jaoui,
743 M., Offenberg, J. H., Kleindienst, T. E., Rubitschun, C., Surratt, J. D., Sheesley, R. J., and Scheller, S.:

744 Secondary organic aerosol formation from fossil fuel sources contribute majority of summertime organic
745 mass at Bakersfield, 117, https://doi.org/10.1029/2012JD018170, 2012.

746 Madejová, J. and Komadel, P.: Baseline studies of the clay minerals society source clays: Infrared
747 methods, Clays and Clay Minerals, 49, 410–432, https://doi.org/10.1346/CCMN.2001.0490508, 2001.

748 Mahalanobis, P., C,: On the generalized distance in statistics, 2, 49–55, 1936.

749 Malm, W. C., Sisler, J. F., Huffman, D., Eldred, R. A., and Cahill, T. A.: Spatial and seasonal trends in
750 particle concentration and optical extinction in the United States, 99, 1347–1370,
751 https://doi.org/10.1029/93jd02916, 1994.

752 Margenot, A. J., Calderón, F. J., Goyne, K. W., Mukome, F. N. D., and Parikh, S. J.: IR Spectroscopy, Soil
753 Analysis Applications, in: Encyclopedia of Spectroscopy and Spectrometry (Third Edition), edited by:
754 Lindon, J. C., Tranter, G. E., and Koppenaal, D. W., Academic Press, Oxford, 448–454,
755 https://doi.org/10.1016/B978-0-12-409547-2.12170-5, 2017.

756 Mayo, D. W., Miller, F. A., and Hannah, R. W.: Course Notes on the Interpretation of Infrared and Raman
757 Spectra, John Wiley & Sons, Hoboken, NJ, 2004.

758 Nemanich, R. J., Lucovsky, G., and Solin, S. A.: Infrared active optical vibrations of graphite, Solid State
759 Communications, 23, 117–120, https://doi.org/10.1016/0038-1098(77)90663-9, 1977.

760 Ngo, M. A., Pinkerton, K. E., Freeland, S., Geller, M., Ham, W., Cliff, S., Hopkins, L. E., Kleeman, M. J.,
761 Kodavanti, U. P., Meharg, E., Plummer, L., Recendez, J. J., Schenker, M. B., Sioutas, C., Smiley-Jewell, S.,
762 Haas, C., Gutstein, J., and Wexler, A. S.: Airborne particles in the San Joaquin Valley may affect human
763 health, 64, 12–16, https://doi.org/10.3733/ca.v064n01p12, 2010.

764 Niyogi, S., Bekyarova, E., Itkis, M. E., McWilliams, J. L., Hamon, M. A., and Haddon, R. C.: Solution
765 Properties of Graphite and Graphene, 128, 7720–7721, https://doi.org/10.1021/ja060680r, 2006.

766 O'Dell, K., Ford, B., Fischer, E. V., and Pierce, J. R.: Contribution of wildland-fire smoke to US PM2.5 and
767 its influence on recent trends, 53, 1797–1804, https://doi.org/10.1021/acs.est.8b05430, 2019.

768 Parks, D. A., Griffiths, P. R., Weakley, A. T., and Miller, A. L.: Quantifying elemental and organic carbon in
769 diesel particulate matter by mid-infrared spectrometry, null, 55, 1014–1027,
770 https://doi.org/10.1080/02786826.2021.1917764, 2021.

771 Reggente, M., Dillner, A. M., and Takahama, S.: Predicting ambient aerosol thermal-optical reflectance
772 (TOR) measurements from infrared spectra: Extending the predictions to different years and different
773 sites, 9, 441–454, https://doi.org/10.5194/amt-9-441-2016, 2016.

https://doi.org/10.5194/amt-2021-382
Preprint. Discussion started: 3 December 2021

Atmospheric Measurement Techniques Discussions

774 Reggente, M., Dillner, A. M., and Takahama, S.: Analysis of functional groups in atmospheric aerosols by
775 infrared spectroscopy: systematic intercomparison of calibration methods for US measurement network
776 samples, Atmos. Meas. Tech., 12, 2287–2312, https://doi.org/10.5194/amt-12-2287-2019, 2019.

777 Russell, L. M., Bahadur, R., and Ziemann, P. J.: Identifying organic aerosol sources by comparing
778 functional group composition in chamber and atmospheric particles, 108, 3516–3521,
779 https://doi.org/10.1073/pnas.1006461108, 2011.

780 Ruthenburg, T. C., Perlin, P. C., Liu, V., McDade, C. E., and Dillner, A. M.: Determination of organic matter
781 and organic matter to organic carbon ratios by infrared spectroscopy with application to selected sites in
782 the IMPROVE network, 86, 47–57, https://doi.org/10.1016/j.atmosenv.2013.12.034, 2014.

783 Savitzky, A. and Golay, M. J. E.: Smoothing and differentiation of data by simplified least squares
784 procedures, 36, 1627–1639, https://doi.org/10.1021/ac60214a047, 1964.

785 Schichtel, B. A., Malm, W. C., Bench, G., Fallon, S., McDade, C. E., Chow, J. C., and Watson, J. G.: Fossil
786 and contemporary fine particulate carbon fractions at 12 rural and urban sites in the United States, 113,
787 https://doi.org/10.1029/2007jd008605, 2008.

788 Senthil Kumar, R. and Rajkumar, P.: Characterization of minerals in air dust particles in the state of
789 Tamilnadu, India through ftir spectroscopy, 2013, 22221–22248, https://doi.org/10.5194/acpd-13-
790 22221-2013, 2013.

791 Snijders, T. A. B. and Bosker, R. J.: Multilevel Analysis: An Introduction to Basic and Advanced Multilevel
792 Modeling, SAGE, 370 pp., 2011.

793 Sorooshian, A., Wonaschütz, A., Jarjour, E. G., Hashimoto, B. I., Schichtel, B. A., and Betterton, E. A.: An
794 aerosol climatology for a rapidly growing arid region (southern Arizona): Major aerosol species and
795 remotely sensed aerosol properties, 116, https://doi.org/10.1029/2011jd016197, 2011.

796 Takahama, S., Schwartz, R. E., Russell, L. M., Macdonald, A. M., Sharma, S., and Leaitch, W. R.: Organic
797 functional groups in aerosol particles from burning and non-burning forest emissions at a high-elevation
798 mountain site, Atmos. Chem. Phys., 11, 6367–6386, https://doi.org/10.5194/acp-11-6367-2011, 2011.

799 Takahama, S., Dillner, A. M., Weakley, A. T., Reggente, M., Bürki, C., Lbadaoui-Darvas, M., Debus, B.,
800 Kuzmiakova, A., and Wexler, A. S.: Atmospheric particulate matter characterization by Fourier transform
801 infrared spectroscopy: a review of statistical calibration strategies for carbonaceous aerosol
802 quantification in US measurement networks, Atmos. Meas. Tech., 12, 525–567,
803 https://doi.org/10.5194/amt-12-525-2019, 2019.

804 Tuinstra, F. and Koenig, J. L.: Raman Spectrum of Graphite, 53, 1126–1130,
805 https://doi.org/10.1063/1.1674108, 1970.

806 Watson, J. G. and Chow, J. C.: A wintertime PM2.5 episode at the Fresno, CA, supersite, Atmospheric
807 Environment, 36, 465–475, https://doi.org/10.1016/S1352-2310(01)00309-0, 2002.

808 Weakley, A. T., Takahama, S., and Dillner, A. M.: Ambient aerosol composition by infrared spectroscopy
809 and partial least-squares in the chemical speciation network: Organic carbon with functional group
810 identification, 50, 1096–1114, https://doi.org/10.1080/02786826.2016.1217389, 2016.

811 Weakley, A. T., Takahama, S., Wexler, A. S., and Dillner, A. M.: Ambient aerosol composition by infrared
812 spectroscopy and partial least squares in the chemical speciation network: Multilevel modeling for
813 elemental carbon, 52, 642–654, https://doi.org/10.1080/02786826.2018.1439571, 2018a.

814 Weakley, A. T., Takahama, S., and Dillner, A. M.: Thermal/optical reflectance equivalent organic and
815 elemental carbon determined from federal reference and equivalent method fine particulate matter
816 samples using Fourier transform infrared spectrometry, 52, 1048–1058,
817 https://doi.org/10.1080/02786826.2018.1504161, 2018b.

818 White, W. H., Trzepla, K., Hyslop, N. P., and Schichtel, B. A.: A critical review of filter transmittance
819 measurements for aerosol light absorption, and de novo calibration for a decade of monitoring on PTFE
820 membranes, 50, 984–1002, https://doi.org/10.1080/02786826.2016.1211615, 2016.

821 Wold, S., Sjöström, M., and Eriksson, L.: PLS-regression: A basic tool of chemometrics, 58, 109–130,
822 https://doi.org/10.1016/S0169-7439(01)00155-1, 2001.

823 Yazdani, A., Dudani, N., Takahama, S., Bertrand, A., Prevot, A. S. H., El Haddad, I., and Dillner, A. M.:
824 Characterization of primary and aged wood burning and coal combustion organic aerosols in an
825 environmental chamber and its implications for atmospheric aerosols, 21, 10273–10293,
826 https://doi.org/10.5194/acp-21-10273-2021, 2021a.

827 Yazdani, A., Dillner, A. M., and Takahama, S.: Estimating mean molecular weight, carbon number, and
828 OM/OC with mid-infrared spectroscopy in organic particulate matter samples from a monitoring
829 network, 14, 4805–4827, https://doi.org/10.5194/amt-14-4805-2021, 2021b.

830 Zhang, X. L., Trzepla, K., White, W., Raffuse, S., and Hyslop, N. P.: Intercomparison of thermal-optical
831 carbon measurements by Sunset and Desert Research Institute (DRI) analyzers using the IMPROVE_A
832 protocol, 14, 3217–3231, https://doi.org/10.5194/amt-14-3217-2021, 2021.

833